Co-pyrolysis of biomass and plastic waste over zeolite- and sodium-based catalysts for enhanced yields of hydrocarbon products

Payam Ghorbannezhad*[a], Sunkyu Park [b], Jude A. Onwudili*[c],

[a] Department of Biorefinery Engineering, Faculty of New Technologies and Energy Engineering, Shahid Beheshti University, Zirab Campus, Mazandaran, Iran.

[b] Department of Forest Biomaterials, College of Natural Resources, NC State University, NC 27695, USA.

[c] European Bioenergy Research Institute, Chemical Engineering and Applied Chemistry, Aston University, Aston Triangle, B4 7ET, Birmingham, United Kingdom.

Abstract

Ex-*situ* co-pyrolysis of sugarcane bagasse pith and polyethylene terephthalate (PET) was investigated over zeolite-based catalysts using a tandem micro-reactor at an optimised temperature of 700 °C. A combination of zeolite (HZSM-5) and sodium carbonate/gamma-alumina served as effective catalysts for 18% more oxygen removal than HZSM-5 alone. The combined catalysts led to improved yields of aromatic (8.7%) and olefinic (6.9%) compounds. Carbon yields of 20.3% total aromatics, 18.3 % BTXE (benzene, toluene, xylenes and ethylbenzene), 17% olefins, and 7% phenols were achieved under optimal conditions of 700 °C, a pith (biomass) to PET ratio of 4 and an HZSM-5 to sodium carbonate/gamma-alumina ratio of 5. The catalytic presence of sodium prevented coke formation, which has been a major cause of deactivation of zeolite catalysts during co-pyrolysis of biomass and plastics. This finding indicates that the catalyst combination as well as biomass/plastic mixtures used in this work can lead to both high yields of valuable aromatic chemicals and potentially, extended catalyst life time.

Keywords: Sugarcane bagasse pith, polyethylene terephthalate (PET), co-pyrolysis, HZSM-5/Na_2CO_3/γ-Al_2O_3 catalysts, hydrocarbons

*Corresponding Authors

(1) Email address: j.onwudili@aston.ac.uk; Tel: +44 (0) 121 204 4703

Postal Address: European Bioenergy Research Institute, Chemical Engineering and Applied Chemistry, Aston University, Aston Triangle, B4 7ET, Birmingham, United Kingdom

(2) Email address: p_ghorbannezhad@sbu.ac.ir; Tel: +98-911-226-6745

Postal Address: Department of Biorefinery Engineering, Faculty of New Technologies and Energy Engineering, Shahid Beheshti University, Zirab, Mazandaran, Iran.

1. Introduction

The impending transition to a low-carbon economy appears immutable and it has been generally accepted that lignocellulosic biomass can play a pivotal role as a valuable renewable resource for the production of biofuels, bio-based chemicals, and biomaterials. Unlike petroleum sources, lignocellulosic biomass can be sustainably grown to be carbon-neutral, enabling mitigation of the effects of greenhouse gases (GHG) emissions. Sugarcane bagasse is one of the most abundant agricultural wastes, with approximately 570 million tonnes generated annually around the world (FAOSTAT, 2018). In tropical and sub-tropical countries, sugarcane bagasse is used for pulp and paper production. However, the presence of pith in the bagasse can cause operational problems (Rainey and Covey, 2016). Sugar cane bagasse contains up to 30 wt% of pith, which is removed during pulp and papermaking because of foaming, increased consumption of cooking chemicals and as well as reduction in paper quality (Chambon et al., 2018). Therefore, the large amounts of pith could be separated and deployed as an abundant and sustainable biomass feedstock for the production of energy and chemicals.

Today, global production of plastics stands at nearly 300 million tonnes per year, a large proportion of this being the so-called single-use plastics, which end up mostly as waste. In 2016 alone, Europe generated more than 25 million tonnes of plastic waste, of which 39% was landfilled (Ratnasari et al., 2017). Among plastic wastes, PET is seen as a problem plastic for thermochemical recyclers because of benzoic acid generation as a major degradation product, which impacts the quality of pyrolysis oil (Diaz-Silvarrey, et al. 2018). The global consumption of PET is nearly 16 million tonnes per year and it is estimated to reach more than 20 million tonnes by 2020 (TCPIE, 2017). Although PET is largely recyclable into fibers, bottles, amorphous PET (APET) sheets and

strapping tape applications, the overall recycling rate of PET is still very low; for example it is less than 10% in the USA (Ko, Sahajwala, and Rawal, 2014).

Therefore, plastic waste and agricultural wastes, such as pith of sugarcane bagasse, are abundant sources for energy and chemical production, which otherwise pose serious disposal problems. The fast pyrolysis is recognized as a more economical and environmentally friendly method to produce biofuel and value-added products (Bridgwater, 2012). The condensed liquid product (bio-oil) can be upgraded, mainly through the removal of oxygenated compounds in order to improve its fuel and chemical properties (Bridgwater, 2012; Wang et al., 2015). Several physical, thermal, chemical and catalytic technologies have been proposed for bio-oil upgrading but these are either expensive or not widely available, and therefore have seen limited commercial interests (Vanderbosch and Prins, 2010). In order to enhance the viability of bio-oil, researchers have suggested co-pyrolysis of biomass and plastics as a potential route (Sharypov et al., 2002; Zhou et al., 2006; Caglar and Aydinli, 2009; Brebu et al., 2010; Pinto et al., 2016). For example, biomass can be co-processed via the catalytic co-pyrolysis with waste plastic using appropriate catalysts (Dorado et al., 2015; Li et al., 2015; Jin et al., 2017; Chattopadhyay et al., 2018; Diaz-Silvarrey, et al. 2018), to produce high-value aromatic (BTXE) chemicals, which are precursor compounds in the pharmaceutical, textile, polymer, automobile, and food industries as well as important additives for gasoline. The world demand for the aromatics including BTXE was valued at $185.9 billion in 2017 (The Business Research Company, 2018).

.

Catalytic fast pyrolysis (CFP) involves the direct conversion of pyrolysis vapours over a catalysts bed without the need for vapour condensation and re-evaporation associated with conventional bio-oil upgrading methods (Carlson et al., 2008; 2011; Cheng et al., 2011; 2012). CFP also avoids the formation of difficult-to-process polymers during bio-oil condensation and storage (Wang, et al., 2012; Elkabasi et al., 2014). Zeolite-based catalysts are effective for promoting the formation of desired aromatic hydrocarbons during catalytic fast pyrolysis (CFP) of plastic-biomass blends (Wang et al., 2013; 2014; Yao et al., 2015; Li et al., 2015). For instance, Zhang et al. (2015), reported a relative content of 20% aromatics from the co-pyrolysis of biomass and plastics at a temperature of 700 °C. However, short catalyst life-time (Wang et al., 2013; 2014, low carbon efficiencies (Yao et al., 2015) and formation of large amounts of char and coke (Yao et al., 2015; Li et al., 2015) are serious technical drawbacks that preclude a cost-effective scale-up of CFP.

Recent research papers (Dorado et al., 2015; Li et al., 2015; Jin et al., 2017; Chattopadhyay et al., 2018; Lu et al., 2018) have revealed an enhancement of aromatic hydrocarbons yields when using HZSM-5 catalysts during the pyrolysis of biomass with aliphatic polymers (PE and PP) and PET. In general, literature has established the positive synergy between biomass and these plastics, resulting in enhanced aromatic carbon yield and reduction of the solid residue (Dorado et al., 2015; Lu et al., 2018). Due to the higher calorific values of plastics compared to biomass, catalytic fast co-pyrolysis of the two feedstocks results in liquids with high energy density (Jin et al., 2017; Chattopadhyay et al., 2018).

Although different studies have been conducted about co-pyrolysis of biomass and plastics over zeolite catalysts, yet the short lifetime of the zeolite catalysts and the formation of coke during the process remain a great challenge. In addition, the optimization of the catalytic biomass – plastic co-pyrolysis process, e.g. with regard to the optimal biomass to catalyst ratio for high yields of

aromatic and olefin compounds is not well understood yet. Thus, the overarching aim of this work is the elucidation of the optimal reaction conditions to achieve high yields of aromatic hydrocarbons compounds and low coke formation during the ex-situ catalytic fast co-pyrolysis of PET and sugarcane bagasse pith using a novel combination of $Na_2CO_3/\gamma\text{-}Al_2O_3$ and HZSM-5 catalysts.

2. Material and methods

2.1 $Na_2CO_3/\gamma\text{-}Al_2O_3$/HZSM-5 catalysts

$Na_2CO_3/\gamma\text{-}Al_2O_3$ catalyst and HZSM-5 catalyst (Si/Al ratio = 23) were purchased from Zeolyst (Netherlands). Before use, the catalysts were treated by calcination at a temperature of 600 °C in a muffle furnace for 5 h. The calcined catalysts were then mixed in different ratios and crushed before sieving to 300 – 500 microns particle size. Five catalysts with different HZSM-5: $Na_2CO_3/\gamma\text{-}Al_2O_3$ ratios of 1:1 to 1:5 were prepared and used for the catalytic pyrolysis of the mixture of the biomass and PET samples.

2.2 Characterisation of sugarcane bagasse pith

The sugarcane bagasse pith used in this study was obtained from the southern part of Iran. It was initially pre-dried under sunlight for two days to decrease its moisture content below 10 wt%. Thereafter, it was further dried in an oven at 105 °C for 2 h. The material was subsequently comminuted to a size of less than 0.3 mm for analytical procedures. Proximate analysis (moisture, volatile matter, fixed carbon, and ash content) and ultimate analysis (carbon, hydrogen, nitrogen, and sulfur), were carried out on the bagasse pith to determine its composition. Proximate analysis was performed using a Perkin Elmer Pyris 1 thermogravimetric analyzer (Shelton, U.S.A). The carrier gas was N_2 at a flow rate of 10 ml/min. Separate samples of bagasse pith and PET were

loaded into the thermo-balance and heated up from 32 to 105 °C at 25 °C/min after which they were kept isothermal at 105°C for 5 minutes. Subsequently, each sample was heated up from 105 to 905 °C at 25 °C/min and held at 905 °C for 15 minutes, before cooling to 200 °C at 25 °C/min. Air was introduced at 20 ml/min and the sample reheated to 575 °C at 100 °C/min and kept at 575 °C for 15 minutes to burn off any remaining char (Ghorbannezhad et al., 2018b).

An adjustment of the ASTM D5373 standard method was used to determine the elemental composition (CHNSO), using an EXETER CE 490 elemental analyzer (ASTM, 2016). Using the ASTM protocols, the ultimate analyses were also performed. Standard methods (TAPPI, 2018) were used to characterise the pith sample for the contents of cellulose (TAPPI, T264 om-88), hemicellulose (TAPPI, T223 om-88), lignin (TAPPI T222 om-88), and acetone or ethanol extractables (TAPPI T 204 om-88).

2.3 Hot water pre-treatment of sugarcane bagasse pith

Due to the process of producing and obtaining sugarcane bagasse pith, it often contains inorganic materials, which may affect the pyrolysis process and influence product yields (Teng et al., 1998; Xue, Braden and Bai, 2017). To remove the inorganics, a hot water pre-treatment procedure was performed, using a water/solid mass ratio of 20 (Ghorbannezhad et al., 2018a). The biomass-water mixture was heated to a temperature of 90°C for 30 min, after which the biomass was washed and dried in an oven at 105°C for 5 h to decrease the moisture content below 10 wt%. The washed sample was subsequently comminuted using a 1 mm hammer mill and sieved to a particle size between 0.25 mm and 1 mm and used for the thermogravimetric analysis and catalytic fast pyrolysis experiments. The biochemical compositions of the pre-treated bagasse pith sample were: 47.8% cellulose, 21.3% hemicellulose, 29.87% lignin and 1.12% extractives.

2.4 Ex-situ catalytic fast pyrolysis experiments

Ex-situ catalytic fast co-pyrolysis experiments of biomass and PET were conducted in a tandem micro-pyrolyzer system (Rx-300 TR, Frontier Laboratories, Japan). The schematic of the experimental setup can be found elsewhere (Wang et al., 2015). Briefly, the system consisted of two independently heated temperature-programmable micro-reactors interfaced to a GC split injection port. One of the micro-reactors was used for pyrolysis while the other contained the catalyst bed for post-pyrolysis reactions of the pyrolysates. For each test, microgram quantities of the biomass/PET mixtures (at different mass ratios) were placed in an 80 µL deactivated stainless steel cup, which then dropped into the 1st reactor for the pyrolysis process at set-point temperatures from 400 to 800 °C. The pyrolysis vapours, was carried by helium flow directly over a fixed bed of catalysts, located in the 2nd downstream quartz-tube micro-reactor held at a fixed temperature of 450 °C. The catalyst bed temperature was selected based on some optimisation experiment using three temperatures in the 400-800°C range (Ghorbannezhad et al., 2018b).

The vapour products leaving the second reactor were fed, via a dedicated interface, into a gas chromatography fitted to a mass spectrometer (GC-MS) for separation and analysis. For the analytical procedure, the injection port was held at 300 °C and the GC oven temperature was initially held at 45 °C for 3 min, then ramped up to 280 °C with a heating rate of 10 °C/min, where it stayed for an additional 6 min, given a total analysis time of 32.5 min. Helium, at a constant flow of 1ml/min, was used as the carrier gas. A split ratio of 1:50 was used each time and all measurements were performed, at least in duplicate to verify the reproducibility of the data. Identification of components was carried out using the NIST10 Library Software installed on the

GC-MS system, while quantification of the yields of identified was determined through calibration with external standards.

Equation (1) was used to calculate the % carbon molar yield of each compound identified and quantified as follows:

$$\% \text{ Molar carbon yield} = \frac{Moles\ of\ carbon\ in\ products}{Moles\ of\ carbon\ in\ feedstock} \times 100 \quad (1)$$

2.5 Optimization by response surface methodology

A central composite design (CCD) methodology was applied to identify and optimise the effects of process conditions on the yield of valuable products. The co-pyrolysis temperature, biomass-to-PET ratio, and HZSM-5-to-γ-Al_2O_3/Na_2CO_3 catalysts ratio were the independent variables. The total aromatics, BTXE, olefins, and phenols yields were set as the dependent variables. A least-square multiple regression methodology was performed to analyze the data using the Design Expert 7 software package (Ghorbannezhad et al., 2018b). The experimental design results were fitted using Eq. 2:

$$Y = \beta_{k0} + \sum_{i=1}^{4} \beta_{ki} x_i + \sum_{i=1}^{4} \beta_{kii} x_i^2 + \sum_{i \neq j=2}^{4} \beta_{kij} x_i x_j \quad (2)$$

Y is the predicted response (product yields); β_{k0}, β_{ki}, β_{kii} and β_{kij} represent regression coefficients; and x_i x_j are the coded independent factors (temperature, biomass to plastic ratio, and HZSM-5 to γ-Na_2CO_3 ratio).

The best model was selected based on the coefficient of determination (R^2), the adjusted coefficient of determination (R^2-adj), the predicted coefficient of determination (R^2-pred), root mean square error of the predictions (RMSEP, see Eq. 3), and the absolute average deviation (AAD). Preferably,

R^2 must be near to 1 and the RMSEP and AAD (see Eq. 4) between the estimated and observed data must be as low as possible (Myers, Montgomery, Anderson-Cook, 2011).

$$\text{RMSEP} = \sqrt{\frac{\sum_{i=1}^{N}(ypre-yexp)2}{N}} \quad (3)$$

$$\text{ADD} = \left\{\sum_{i=1}^{N}(|\text{yexp} - \text{ypre}|/\ \text{yexp})\ /N\right\} \times 100 \quad (4)$$

Y_{pre}, Y_{exp}, and N are the predicted data, observed data, and the number of treatments, respectively. The significant model of lack of fit indicates the equation of fitting is suitable to characterize the results. All equations were obtained after elimination. After selecting the most accurate model, the analysis of variance (ANOVA) was used to determine the statistical significance of the regression coefficients by conducting a Fisher`s F-test at 95% confidence level. The interactive effects of the factors were observed using surface plots, derived from the chosen model (Ghorbannezhad et al., 2016). Finally, the process was optimized, with the aim of maximizing the aromatics, BTXE, olefins, and phenols yields with the same weight (w = 1) and the credibility of the optimum conditions was diagnosed through the desirability values of the responses which ranged from 0 to 1. The closer values of desirability to 1 showed the more desirable and credible optimal conditions. In this study, after the optimum point was obtained with the CCD software, the samples were tested at this optimum point by laboratory experiments to obtain the results presented here. Furthermore, these results were validated by a control experiment under the predicted optimum conditions.

3. Results and discussion

3.1 Elemental analysis

The elemental compositions of bagasse pith and PET are presented in Table 1. One of the main parameters for biomass characterisation is water content. The efficiency of the pyrolysis process

is significantly reduced when moisture content is above 10 wt% (Bridgwater, 2012) and results in Table 1 showed that the biomass was successfully dried to below 10 wt% moisture content prior to pyrolysis in this work. The pith of sugarcane bagasse contained the high volatile matter (72 wt%) which indicated the capability of its devolatilisation. The characterisation of sugarcane bagasse pith showed that it also contained substantial amounts of extractives and inorganic matter, especially Ca, K, and Mg (Table 1). The inorganic compounds required attention due to their catalytic activities, which could adversely affect the bio-oil yield and increase char formation during the pyrolysis process (Xue, Braden and Bai, 2017). Thus, the pre-treatment of fresh pith was essential to eliminate inorganic materials, without significant effects on the main biomass components.

Table1. Ultimate and Proximate analysis of Pith of bagasse and PET

Component	**Weight%**		**Standard method**
	Bagasse pith	PET	
Proximate Analysis (wt%, db*)			
Moisture	10	0.5	ASTM D 3173
Volatile	72	97.8	ASTM 3174
Fixed carbon	16.1	1.59	ASTM 3175
Ash	1.9	0.1	ASTM 3172
Ultimate Analysis (wt%, daf)**			
C	39.15	57.9	ASTM D 4239
H	5.35	4.13	ASTM D 4239
N	0.36	0.16	ASTM D 4239
S	0.01	0.01	ASTM D 4239
O	55.14	37.7	By difference
Inorganic Compounds (ppm, db*)			
Ca	19110	-	ASTM D 5373
Mg	3513	13.5	ASTM D 5373
K	3139	-	ASTM D 5373
Al	3596	217	ASTM D 5373
Si	18350	-	ASTM D 5373

*db = dry basis; **daf = dry ash-free basis,

3.2 Thermogravimetric analysis (TGA)

Fig. 1 shows the TGA and DTG curves of the thermal and non-catalytic degradation of the individual pith and PET samples at a heating rate of 20 °C/min. For pith biomass, the first stage started at room temperature and continued up to 100 °C with 10% weight loss, which is moisture evaporation, followed by maximum weight loss of 60% observed from 250 to 350 °C due to a progressive degradation of hemicellulose, cellulose, and lignin.

In contrast to pith, the PET exhibited maximum mass loss at a higher temperature of 400-575 °C, where it levelled-off but continued its degradation up to 700 ºC. These results were similar to previous studies on the co-pyrolysis of biomass and plastics (Li et al., 2013; Ratnasari et al., 2017). It was anticipated that the mixture of biomass and PET would present different degradation patterns. In addition, catalysts (e.g. zeolites) could change the thermal decomposition profile of the mixed pith and PET, by influencing the interactions among volatile components released from the materials during pyrolysis. The catalytic activity could be interrupted by the effect of biomass decompositions products, by deactivating the acidic zeolite sites and delay the catalytic reactions of the plastics (Zhang et al., 2012). Literature shows that co-pyrolysis of biomass and plastic mixtures are carried out above the normal biomass pyrolysis temperature of 500 ºC due to the technical problem of the presence of heavy hydrocarbons in the resulting oil product. Hence, a potential solution to this problem is to operate co-pyrolysis systems at temperatures of 700 ºC and above (Lin et al., 2015; Uzoejinwa et al., 2018). Therefore, based on results from TGA/DTG studies and literature sources, it was decided to carry out the co-pyrolysis tests at 700 ºC, with the validation of the optimised parameters in *Section 3.6.*

3.3 Non -catalytic fast co-pyrolysis of PET and pith

The non-catalytic fast pyrolysis of pith and PET was first performed using the Py-GC-MS. Figs. 2a and 2b present the chromatograms from the non-catalytic tests, illustrating the distribution of products derived from separate components of pith and PET. Without the HZSM-5, the pith of sugarcane bagasse decomposed into a distribution of different oxygenates as a result of the breakdown of cellulose, hemicellulose, and lignin, while a mixture of hydrocarbons (alkenes and alkanes) is liberated from the thermal decomposition of the long hydrocarbon chain structure of PET. Anhydrosugars like levoglucosan, furans, alcohols, and ketones were the main products for the non-catalytic pyrolysis of pith, similar to those reported elsewhere (Ghorbannezhad et al., 2018a, 2018b).

3.4. Catalytic fast co-pyrolysis of PET and pith

As can be seen from the chromatograms in Fig. 2c, catalytic pyrolysis of pith over HZSM-5 predominantly decreased the content of oxygenated compounds and increased the yields hydrocarbons. The compounds identified were similar to those reported in literature (Karagoz et al, 2016; Ghorbannezhad et al, 2018) and included furan, benzene, toluene, xylenes, ethylbenzene, indenes, and naphthalene, which were totally different from the products of non-catalytic fast pyrolysis. Catalysts can therefore enable the change in type, yield, and distribution of products during fast pyrolysis process.

While, it is worth noting that catalytic fast pyrolysis of biomass is a method to produce deoxygenated pyrolysis liquids, it is still a low-efficiency process because catalytic mechanisms lead to loss of hydrogen (mainly as water via dehydration) from the biomass, leading to

condensation of carbon atoms to form coke and consequently causing catalyst deactivation, which shortens catalyst life-time. The oxygenated compounds in bio-oil or pyrolysis vapours are known to undergo severe thermal degradation on solid acid catalysts, resulting in the formation of carbonaceous deposits on the catalyst, and consequently, lead to an intense deactivation of the catalyst (Sebestyne, et al, 2017). Zhang et al. (2015) also reported that the higher catalyst deactivation occurred at a lower H/C_{eff} ratio of biomass feedstock which resulted in reduction of aromatics yields. The loss of hydrogen can be compensated by mixing plastic as a hydrogen-enriched reactant. HZSM-5 being a shape-selective acidic catalyst, can convert the anhydrosugars into smaller molecules, such as furans, HMF, aldehydes, and other acids through carbocation formation on the external surface acid sites of the catalyst (Speight, 1991). In addition, aromatic formation has been reported to occur with Brønsted sites of HZSM-5 through a "hydrocarbon pool", in which aromatic hydrocarbons formed inside the zeolite pores as a result of catalysed conversion of oxygenated compounds (Dorado et al., 2015). Regarding the aromatization reaction pathway, some studies generally have confirmed the following steps: a) cracking and deoxygenation of biomass into small C2−C5 olefins; b) oligomerization of C2−C5 olefins to C6−C10 olefins, followed by transformation to C6−C10 dienes by transfer reactions; c) aromatization of the dienes (Mullen and Boateng, 2015; Hoff et al., 2016).

Hoff et al. (2016) revealed that aromatics formation was strongly dependent on the crystallinity and accessibility of framework aluminum sites over zeolite-based catalysts. However, the same mechanisms are responsible for rapid deactivation of zeolite catalyst from coke formation (Mullen and Boateng, 2015). Therefore, to improve catalysts' lifetime and reduce the formation of coke, the use of specific sodium-based catalytic additives can be an interesting option because this

specific material offers large pores (microporous), giving better access for large and bulky molecules and thus enhancing the catalytic conversion to aromatics.

3.5 Catalytic co-pyrolysis over sodium-based catalyst

The chromatogram in Figure 2d shows that the co-pyrolysis of biomass and PET over the combined HZSM-5/γ-Na_2CO_3 catalysts enhanced the selectivity of aromatic hydrocarbons in the liquid product. Such a synergistic effect between PET and bagasse during the co-pyrolysis could both improve the aromatics and reduce the coke formation (Dorado et al., 2015; Li et al., 2013; 2014). Hence to test this hypothesis, a quick set of experiments was carried out to evaluate the effect of increasing PET/biomass ratio on coke formation in the absence of catalyst. The results are shown in *Supplementary Information Fig. SI1*, indicating that coke formation reduced with increasing PET in the plastic/biomass blend, indicating that the plastic could prevent coke formation. The reduction of coke formation during catalytic co-pyrolysis of biomass and PET can help to extend the HZSM-5 life-time and further enhance the yields of the desired products. This will be the subject of future research.

Fig. 3 presents the total yields of the aromatic hydrocarbon products from the co-pyrolysis of pith at 700 ^{o}C with PET using a biomass/PET ratio of 4 and an HZSM-5/γ-Al_2O_3/Na_2CO_3 of 5. The cumulative amount of carbon in the aromatic products was around 22%. The transfer of hydrogen from PET-derived aliphatics toward the lignin-derived oxygenated compounds could mitigate polymerization and cross-linking char forming reactions. In fact, using PET as a hydrogen-rich plastic appeared to support the 'hydrocarbon pool' pathway, ensuring that the oxygenated primary pyrolysis products of biomass do not cause coke formation. Results also showed that H_2O

formation decreased, leading to an increase in aromatic compounds. The major aromatic compounds obtained were ethylbenzene, toluene, and xylenes.

In addition to the 'hydrocarbon pool' pathway, aromatics formation during pyrolysis can occur via the Diels-Alder cycloaddition of olefin gases (ethylene and propylene) and furan derivatives over zeolite catalysts (Cheng and Huber, 2011). Hence, it is possible that the reactions between olefin gases from PET and furans from pith, could have occurred in this study, leading to enhanced yields of aromatic hydrocarbons such as benzene, toluene, and xylenes (Cheng et al., 2012). A plausible schematic of aromatic hydrocarbon production via the combination of the hydrocarbon pool pathway and the Diel-Alder reactions from the co-pyrolysis of biomass and plastic is illustrated in Fig. 4.

The catalysts seemed to have intensified the secondary reactions of organic components involving C−C, C−O, and C−H bond cleavage during CFP. It would appear that the Na_2CO_3 improved the deoxygenating rate and life-time of the zeolite catalysts by reducing surface coke formation, which can be favourable towards the scale-up of the CFP process. Enhanced deoxygenation rate during in-situ catalytic fast pyrolysis of Jatropha seed cake using Na_2CO_3 as catalyst has been reported by Imran et al. (2016). In their study, the catalyst was mixed in a bench-scale entrained flow reactor setup and resulted in an upgraded bio-oil with very low oxygen and water contents (7.1 and 6.8 wt.%, respectively), due to removal of undesirable compounds, i.e., acids and aldehydes. Consequently, there oil product showed a dramatic increase in the aliphatic and aromatic hydrocarbons content (Imran et al., 2016). It has been also observed that the sodium-based catalysts like $Na_2CO_3/\gamma\text{-}Al_2O_3$ were the most active for deoxygenation of pyrolysis products (Nguyen et al., 2013). In this present work, the decrease in oxygen content was accompanied by a

dramatic increase in CO_2 production during the Py-GC-MS experiment (Fig. 2d). The selectivity of oxygenated compounds toward CO_2 is desirable in biomass deoxygenation to minimize hydrogen loss. Nguyen et al. (2016) revealed that carboxylic acids were completely removed, and hydrocarbon content significantly increased in the presence of the $Na_2CO_3/\gamma\text{-}Al_2O_3$ catalyst. Nguyen et al. (2015) proposed the conversion of carboxylic acids over $Na_2CO_3/\gamma\text{-}Al_2O_3$ occurred via the ketonisation of carboxylic acids, with subsequent decarboxylation/dehydration over HZSM-5 into olefins. However, the catalyst was reported to have suffered from agglomeration and loss of activity. However, chemical interaction or agglomeration of HZSM-5 and $Na_2CO_3/\gamma\text{-}Al_2O_3$ catalysts have not been determined in this present study.

3.6 Optimization of catalytic co-pyrolysis process over sodium-based HZSM5 catalyst mixture

As shown in Fig. 5, the independent effect of the HZSM-5 to $Na_2CO_3/\gamma\text{-}Al_2O_3$ ratio was investigated to achieve preliminary optimisation of valuable co-pyrolysis products (aromatics, BTXE, olefins, and phenols). The effect of the HZSM-5 addition was established within the range of a 1 to 5 ratio relative to pith (biomass) in this study. The effect of changing the HZSM-5/ $Na_2CO_3/\gamma\text{-}Al_2O_3$ ratio was more pronounced in the yields of phenols compared to BTXE. An HZSM-5 to the $\gamma\text{-}Na_2CO_3$ ratio of 4 gave the highest phenols yield as shown in Fig. 5.

In comparison with the effects of the HZSM-5 to $Na_2CO_3/\gamma\text{-}Al_2O_3$ ratio, the biomass to PET ratio showed a greater effect on the yield of valuable co-pyrolysis products (Fig. 6). For instance, the BTXE yield increased by increasing the biomass to PET ratio, while an increase in HZSM-5 to $Na_2CO_3/\gamma\text{-}Al_2O_3$ did not show significant effects. The optimal biomass to PET was determined at a ratio of 4 when the maximum aromatics, BTXE, olefins, and phenols were obtained at carbon

yields of around 22%, 19%, 17%, and 7 %, respectively (Fig. 6). The independent effect of biomass to PET revealed that the phenols also exhibited the most significant changes in co-pyrolysis valuable products, relative to changes in BTXE and aromatics. However, the total yields of phenols were much lower compared to BTXE.

Fig. 7 shows the aromatics and BTX efficiency by evaluating several parameters such as biomass to PET ratio, HZSM-5 to $Na_2CO_3/\gamma\text{-}Al_2O_3$, and temperature on the co-pyrolysis process. It can be ascertained from Fig. 7 that the combination of HZSM-5 and $Na_2CO_3/\gamma\text{-}Al_2O_3$ catalyst was the most effective parameter, resulting in 18% oxygen removal and 19% of BTX yields than either HZSM-5 or $Na_2CO_3/\gamma\text{-}Al_2O_3$ alone. This could be attributed to the enhanced co-pyrolysis process due to more deoxygenation and formation of aromatic as well as reduction of coke. Ghorbannezhad et al. (2018b) indicated that the highest BTX compounds were obtained when using HZSM-5 with a Si/Al ratio of 23. They reported that the increased cracking reaction of the primary pyrolysis products taking place on the HZSM-5 zeolite catalyst could be attributed to the acidic nature of HZSM-5.

Zhang et al. (2016) reviewed the co-pyrolysis performance which can be influenced by process parameters like temperature, type of catalysts, and the ratio of co-reactants on the liquid products. Nguyn et al. (2015) proposed that the coordination of Na^+ ions and the hydroxyl and alkoxyl groups on the surface of $Na_2CO_3/\gamma\text{-}Al_2O_3$ was responsible for improving deoxygenation which corresponded to higher number of sodium active sites. On the other hand, the pivotal role of sodium concentrations rather than the surface area of catalysts resulted in the lignin-derived compounds being promoted through catalytic scission of these groups over $Na_2CO_3/\gamma\text{-}Al_2O_3$ catalyst.

Based on the statistical analysis, the full quadratic model was selected as the best model and biomass to PET ratio was shown to have the most significant effect on the aromatic compounds yields and coke formation. The optimal yields of BTXE (18.3%) and total aromatic compounds (20.3%) were obtained at a temperature of 700 °C, biomass to PET ratio of 4, and HZSM-5 to $Na_2CO_3/\gamma\text{-}Al_2O_3$ ratio of 5. To validate the optimisation results, additional experiments with three replications were carried out at the optimum situation. It was observed that the BTXE yield (18.3% ± 1.04), aromatics (20.3% ± 0.79), olefins (17% ± 0.65) and phenols (7% ± 0.23) were close to the predicted values ($P < 0.05$), which indicated the high accuracy of the presented models.

4. Conclusions

This study has revealed that the co-pyrolysis of sugarcane bagasse pith with PET, using an *ex-situ* Py-GC-MS, increased the production of aromatic compounds, especially BTXE and minimized the formation of coke. Results indicated that the PET strongly influenced the thermal decomposition of lignin in pith during the co-pyrolysis study. This implied that the transfer of hydrogen from PET-derived aliphatics toward the lignin-derived oxygenated compounds could mitigate polymerisation and cross-linking char forming reactions. In addition, dehydration reactions that generate H_2O are suppressed. Moreover, the combination of sodium-based catalyst ($Na_2CO_3/\gamma\text{-}Al_2O_3$) with HZSM-5 improved the deoxygenation reactions, while reducing coke formation. Optimisation of ex-situ co-pyrolysis indicated that the maximum yields of aromatic compounds were obtained at 700 °C, biomass to PET ratio of 4, and HZSM-5 to $Na_2CO_3/\gamma\text{-}Al_2O_3$ ratio of 5. At these conditions, an optimum BTX yield of 18.3% was obtained. Finally, this present study showed that catalytic fast pyrolysis technology can be deployed to reduce the disposal of

waste plastics in landfills, reduce our dependence of fossil fuels, and introduced new pyrolysis-based biorefinery pathways in chemical industries.

Acknowledgments

This study was supported partially by the ENgineering and TEchnology Institute Groningen (ENTEG) and Department of Chemical Engineering (award number: 190138720) and Department of Biorefinery Engineering at Shahid Beheshti University, Iran (award number: 397081).

References

ASTM D5373-16, 2016. Standard Test Methods for Determination of Carbon, Hydrogen, and Nitrogen in Analysis Samples of Coal and Carbon in Analysis Samples of Coal and Coke, ASTM International, West Conshohocken, PA.

Bridgwater, A.V., 2012. Review of fast pyrolysis of biomass and product upgrading. Biomass Bioenerg. 38, 68–94.

Brebu, M., Ucar, S., Vasile, C., Yanik, J. 2010. Co-pyrolysis of pine cone with synthetic polymers. Fuel 89, 1911-1918.

Caglar, A., Aydinli, B. J. 2009. Isothermal co-pyrolysis of hazelnut shell and ultra-high molecular weight polyethylene: The effect of temperature and composition on the amount of pyrolysis products, J. Anal. Appl. Pyrolysis 86, 304−309.

Carlson, T.R, Vispute, T. P. and Huber, G. W. 2008. Green gasoline by catalytic fast pyrolysis of solid biomass-derived compounds. ChemSusChem 1 (5), 397–400.

Carlson, T. R, Cheng, Y.-T., Jae, J. Huber, G. W. 2011. Production of Green Aromatics and Olefins by Catalytic Fast Pyrolysis of Wood Sawdust, Energ. Environ. Sci. 4, 145-161.

Chambon, C.L., Mkhize, T.Y., Reddy, P., Brandt‐Talbot, A., Deenadayalu, N., Fennell, P.S. and Hallett, J.P., 2018. Pretreatment of South African sugarcane bagasse using a low‐cost protic ionic liquid: a comparison of whole, depithed, fibrous and pith bagasse fractions. Biotechnol. Biofuels 11, 247-262.

Chattopadhyay, J., Pathak, T.S., Srivastava, R., Singh, A.C. 2018. Catalytic co-pyrolysis of paper biomass and plastics mixtures, HDPE, PP and PET, and product analysis. Energy 103, 513-521.

Cheng, Y.-T., Huber, G. W. 2011. Chemistry of Furan Conversion into Aromatics and Olefins over HZSM-5: A Model Biomass Conversion Reaction. ACS Catal. 1(6), 611-628.

Cheng, Y. T., Jae, J., Shi, J., Fan, W., Huber, G. W., 2012. Renewable Aromatics Production by Catalytic Fast Pyrolysis of Lignocellulosic Biomass with Bifunctional Ga/ZSM-5 Catalysts. Angew. Chem. Int. Edit. 51, 1387–1390.

Diaz-Silvarrey, L., McMahan, A., Phen, A.N. 2018. Benzoic acid recovery via waste poly (ethylene terephthalate) (PET) catalytic pyrolysis using a solphated zirconia catalyst. J. Anal. Appl. Pyrol. 134, 621-631.

Dorado, C., Mullen, C. A., Boateng, A. A. 2015. Origin of carbon in aromatic and olefin products derived from HZSM-5 catalyzed co-pyrolysis of cellulose and plastics via isotopic labeling. Appl. Catal. B- Environ. 162, 338–345.

Dorado, C., Mullen, C. A., Boateng, A. A. 2014. H-ZSM5 catalyzed the co-pyrolysis of biomass and plastics. ACS Sustain. Chem. Eng. 2, 301−311.

Elkasabia, Y., Mullen, C.A., Pighinelli, A.L.M.T., Boateng, A.A., 2014. Hydrodeoxygenation of fast-pyrolysis bio-oils from various feedstocks using carbon-supported catalysts. Fuel Proc. Technol. 123, 11–18

FAOSTAT, 2018. Statistic Report, crops, http://www.fao.org/faostat/en/#data/QC/visualize. Accessed November 10, 2018.

Ghorbannezhad, P., Dehghani, M.R., Ghasemian, A., Wild, P., Heeres, J.H. 2018. Sugarcane bagasse ex-situ catalytic fast pyrolysis for the production of Benzene, Toluene, and Xylenes (BTX), J. Anal. Appl. Pyrol, 131, 1–8.

Ghorbannezhad, P., Dehghani, M.R., Ghasemian, A. 2018. Catalytic fast pyrolysis of sugarcane bagasse pith with HZSM-5 catalyst using tandem micro-reactor-GC-MS. Energy. Source. Part A 40(1), 15–21.

Ghorbannezhad, P., Bay, A., Youlmeh, M., Yadollahi, R., Moghadam, Y.J., 2016. Optimization of coagulation-flocculation process for medium density fiberboard (MDF) wastewater through response surface methodology. Desalin. Water Treat. 1–16.

Heikkienen, J.M., Hordijk, J., de Jong, W., Spliethoff, H. 2004. Thermogravimetry as a tool to classify waste components to be used for energy generation. J. Anal. Appl. Pyrol. 71, 883-900.

Hoff, T., Gardner, D.W., Thilakaratne, R., Wang, K., Hansen, T.W., Brwon, R.C., Tessonnier, J.P. 2016. Tailoring ZSM-5 zeolites for the fast pyrolysis of biomass to aromatic hydrocarbons. ChemSusChem 9, 1473-1482.

Imran, A., Bramer, E.A., Seshan, K., Brem, G., 2016. Catalytic flash pyrolysis of oil impregnated-wood and jatropha cake using sodium-based catalysts. J. Anal. Appl. Pyrolysis. 117, 236-246.

Jin, Q., Wang, X., Li, S., Mikulicic, H., Besenic, T., Deng, S., Vujanovic, M., Tan, H., Kumfer, B. 2017. Synergic effects during co-pyrolysis of biomass and plastics: Gas, Tar, Soot, Char products, and thermogravimetric study. J. Energy. Inst, https://doi.org/10.1016/j.joei.2017.11.001

Karagoz, S., Kawakami, T., Kako, A., Liguni, Y., Ohtani, H. 2016. Single shot pyrolysis and on-line conversion of lignocellulosic biomass with HZSM-5 catalyst using tandem-micro-reactor-GC-MS, RSC advances, 6, 46108-46115.

Ko, K.H., Sahajwalla, V., Rawal, A. 2014. Specific molecular structure changes and radical evolution during biomass-polyethylene terephthalate co-pyrolysis detected by (13)C and (1)H solid-state NMR. Biores. Technol. 170, 248-255.

Li, J., Yu, Y., Li, X., Wang, W., Yu. G., Deng, S., Huang, J., Wang, B., Wang, Y., 2015. Maximizing carbon efficiency of petrochemical production from catalytic co-pyrolysis of biomass and plastics using gallium-containing MFI zeolites. Appl. Catal. B: Environ. 172–173, 154–164.

Li, X.; Li, J.; Zhou, G.; Feng, Y.; Wang, Y.; Yu, G.; Deng, S.; Huang, J.; Wang, B. 2014. Enhancing the production of renewable petrochemicals by co-feeding of biomass with plastics in catalytic fast pyrolysis with ZSM-5 zeolites. Appl. Catal. A: General 481, 173−182.

Li, X.; Zhang, H.; Li, J.; Su, L.; Zuo, J.; Komarneni, S.; Wang, Y. 2013. Improving the aromatic production in catalytic fast pyrolysis of cellulose by co-feeding low-density polyethylene. Appl. Catal. A: General 455, 114−121.

Lin, X., Zhang, Z., Sun, J., Guo, W, Wang, Q., 2015. Effects of phosphorus-modified HZSM-5 on distribution of hydrocarbon compounds from wood–plastic composite pyrolysis using Py-GC/MS. J. Anal. Appl. Pyrol. 116, 223 -230.

Lu, P., Hung, Q., Bourtsalas, A.C., Chi, Y., Yan, J. 2018. Synergistic effect on char oil produced by the co-pyrolysis of pinewood, polyethylene, and polyvinyl chloride. Fuel 230, 359-367.

Marin, N.; Collura, S.; Sharypov, V. I.; Beregovtsova, N. G.; Baryshnikov, S. V.; Kutnetzov, B. N.; Cebolla, V. L.; Weber, J. V. 2002. Co-pyrolysis of wood biomass and synthetic polymers mixtures. Part II: characterization of the liquid phases. J. Anal. Appl. Pyrol. 65 (1), 41−55.

Myers, R.H., Montgomery, D.C., Anderson-Cook, C.M., 2011. Response Surface Methodology: Process and product optimization using designed experiments. John Wiley & Sons, New York, NY, (3rd Edition).

Mullen, C.A., Boateng, A.A. 2015. Production of aromatic hydrocarbons via catalytic pyrolysis of biomass over Fe-Modified HZSM-5 zeolites. ACS Sustain. Chem. Eng. 3, 1623–1631.

Nguyen, T.S., He, S, Raman, G., Seshan, K. 2016. Catalytic hydro-pyrolysis of lignocellulosic biomass over dual Na_2CO_3/Al_2O_3 and Pt/Al_2O_3 catalysts using n-butane at ambient pressure. Chem. Eng. J. 299, 415–419.

Nguyen, T.S., Lefferts, L., Gupta, S.K., Seshan, K. 2015. Catalytic conversion of biomass pyrolysis vapors over sodium-based catalyst: A study on the state of sodium on the catalyst. ChemCatChem 7, 1833 – 1840.

Nguyen, T.S, Zabeti, M., Lefferts, L, Brem, G, Seshan, K. 2013. Catalytic upgrading of biomass pyrolysis vapours using faujasite zeolite catalysts. Biomass Bioenerg. 48, 100-110.

Pinto, F., Miranda, M., Costa, P. 2016. Production of liquid hydrocarbons from rice crop wastes mixtures by co-pyrolysis and co-hydropyrolysis. Fuel 174 (15), 153–163.

Ratnasari, D. K., Nahil, M. A., Williams, P. T. 2017. Catalytic pyrolysis of waste plastics using staged catalysis for the production of gasoline range hydrocarbon oils. J. Anal. Appl. Pyrol. 124, 631–637.

Rainey, T. J., and Covey, G., 2016. Pulp and paper production from sugarcane bagasse. In O'Hara, I. M. and Sagadevan, M. (Eds.) Sugarcane-based Biofuels and Bioproducts. John Wiley & Sons Inc, Hoboken, New Jersey, 259-280.

Sharypov, V. I., Marin, N., Beregovtsova, N. G., Baryshnikov, S.V., Kuznetsov, B. N., Cebolla, V. L., Weber, J. V. 2002. Co-pyrolysis of wood biomass and synthetic polymer mixtures. Part I: influence of experimental conditions on the evolution of solids, liquids, and gases. J. Anal. Appl. Pyrol. 64, 15−28.

Sebestyen, Z., Barta-Rajna, E., Bozi, J., Blazso, M., Jakab, E., Miskolezi, N., Soja, J., Czegeny, Zs. 2017. Thermo-catalytic pyrolysis of biomass and plastic mixtures using HZSM-5, Applied Energy, 207, 114-122.

Speight, J. G., 1991. Refining Chemistry. In The Chemistry and Technology of Petroleum, 2nd ed., revised and expanded; Heinemann, H., Ed.; Chemical Industries Series; Marcel Dekker, Inc., New York, 44, 473−497.

TAPPI, 2018. TAPPI Standards: Regulations and Style Guidelines. Norcross, GA 30024, USA

T.C.P.I.E. Office, 2017. Progress of the World's Plastics Industry in 2014-2015, China Plastics Industry, 44, 46

Teng, H. and Wei, Y.C., 1998. Thermogravimetric studies on the kinetics of rice hull pyrolysis and the influence of water pretreatment. Ind. Eng. Chem. Res. 37(10), 3806-3811.

The Business Research Company, 2018. Aromatics Global Market Briefing 2018. Accessed July 31, 2019.

Uzoejinwa, B.B., He, X., Wang, S., Abomohra, A. E-F., Hu, Y., Wang, Q., 2018. Co-pyrolysis of biomass and waste plastics as a thermochemical conversion technology for high-grade biofuel production: Recent progress and future directions elsewhere worldwide. Energy Con. Mgt, 163, 468-492

Vanderbosch, R.H., Prins, W. 2010. Fast pyrolysis technology development. Biofuel. Bioprod. Bior. 4(2), 178-208.

Wang, Y., He, T., Liu, K., Wu, J., Fang, Y., 2012. From biomass to advanced bio-fuel by catalytic pyrolysis/hydro-processing: Hydrodeoxygenation of bio-oil derived from biomass catalytic pyrolysis. Biores. Technol. 108, 280–284

Wang, K., Zhang, J., Shanks, B.H., Brown, R.C. 2015. Catalytic conversion of carbohydrate-derived oxygenates over HZSM-5 in a tandem micro-reactor system, Green Chem. 17, 557-564.

Wang, K., Kim, K. H, Brown, R. C. 2014. Catalytic pyrolysis of individual components of lignocellulosic biomass. Green Chem. 16, 727-735.

Wang, L., Lei, H., Lee, J., Chen, S., Tang, J., Ahring, B. 2013. Aromatic hydrocarbons from packed-bed catalysis coupled with microwave pyrolysis of Douglas fir sawdust pellets. RSC Advances 34 (3), 14609–14615.

Xue, Y., Braden, J. and Bai, X., 2017. Effect of Pretreatment on biomass pyrolysis for better quality of bio-oil. Proceedings of the AIChE Annual Meeting, October 2017. Indianapolis, USA.

Yao, W., Li, J., Feng, Y., Wang, W., Zhang, X., Chen, Q., Komarneni, S., Wang, Y. 2015. Thermally stable phosphorus and nickel modified ZSM-5 zeolites for catalytic co-pyrolysis of biomass and plastics. RSC Advances 5, 30485–30494.

Zhang, X., Lei, H., Chen, S., and Wu, J., 2016. Catalytic co-pyrolysis of lignocellulosic biomass with polymers: a critical review. Green Chem. 18, 4145-4169

Zhang, B., Zhong, Z., Ding, K., Song, Z. 2015. Production of aromatic hydrocarbons from catalytic co-pyrolysis of biomass and high-density polyethylene: Analytical Py−GC/MS study. Fuel 139, 622−628.

Zhang, H., Carlson, T. R., Xiao, R., Huber, G. W. 2012. Catalytic fast pyrolysis of wood and alcohol mixtures in a fluidized bed reactor. Green Chem. 14, 98−110.

Zhou, L.; Wang, Y.; Huang, Q.; Cai, J. 2006. Thermogravimetric characteristics and kinetic of plastic and biomass blends co-pyrolysis, Fuel. Process. Technol. 87 (11), 963−969.

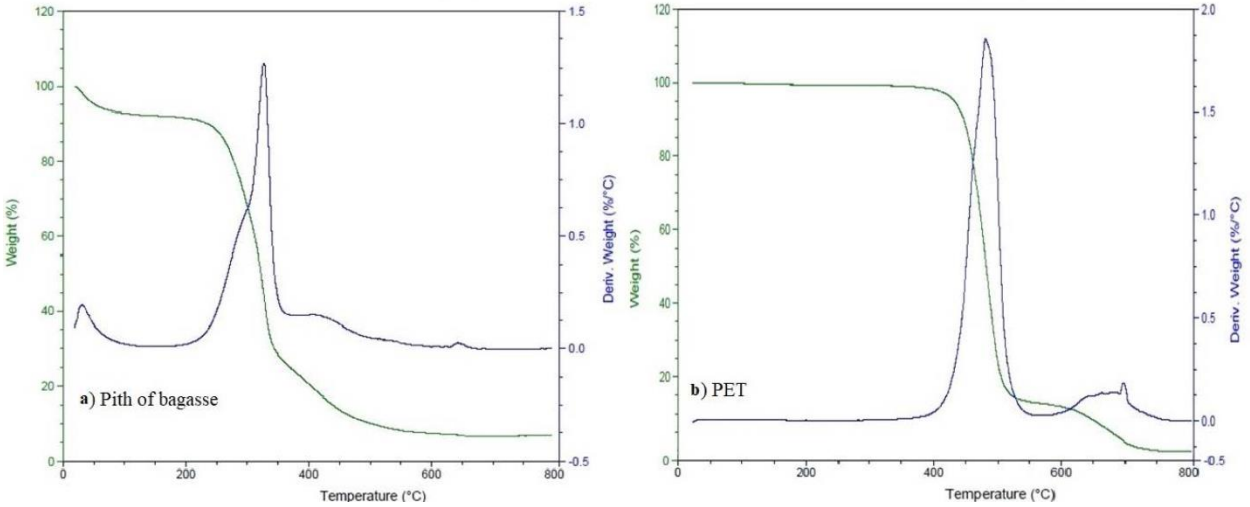

Fig. 1. TGA and DTG analysis, a) Pith of bagasse and b) PET

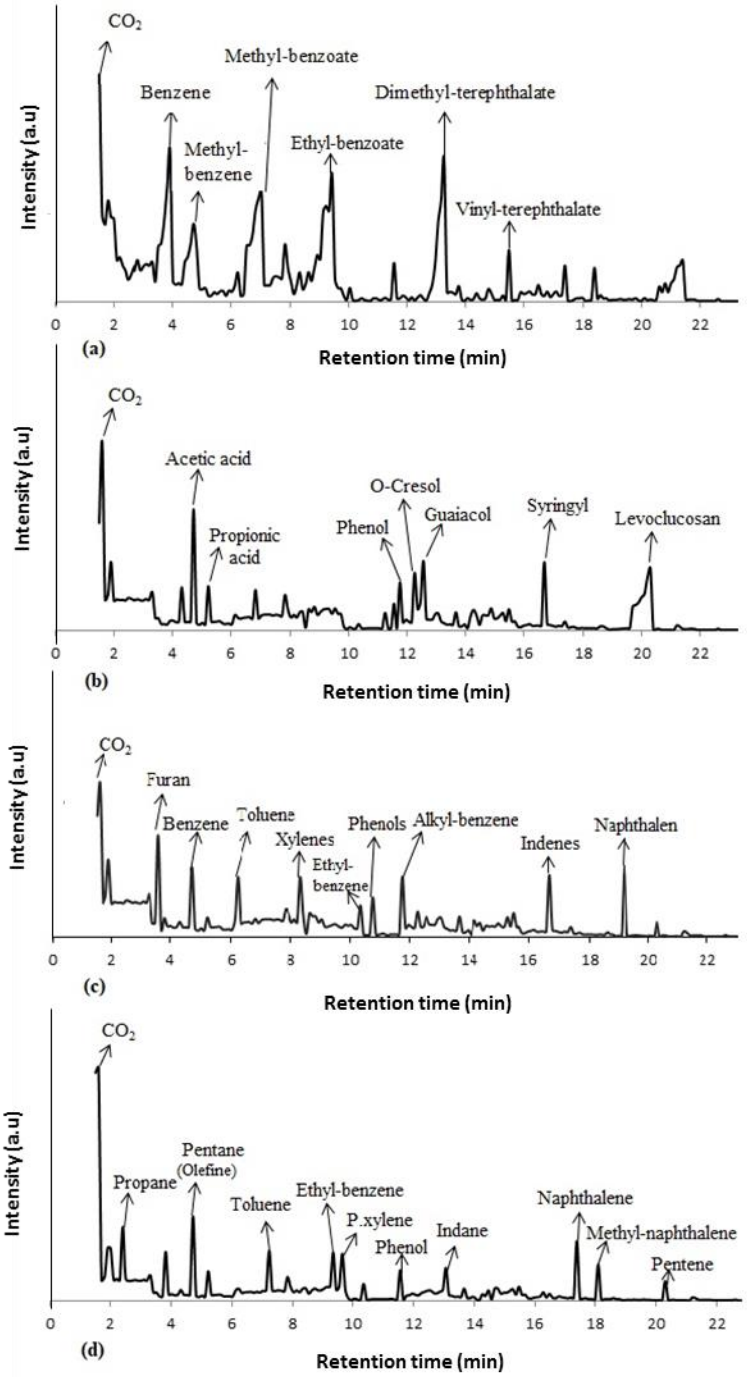

Fig. 2. Py-GC-MS chromatography for, a) PET; b) pith of bagasse; c) Pith of bagasse with HZSM-5 catalyst; d) Co-pyrolysis of pith of bagasse with PET over HZSM-5/γ-Na_2CO_3 catalyst

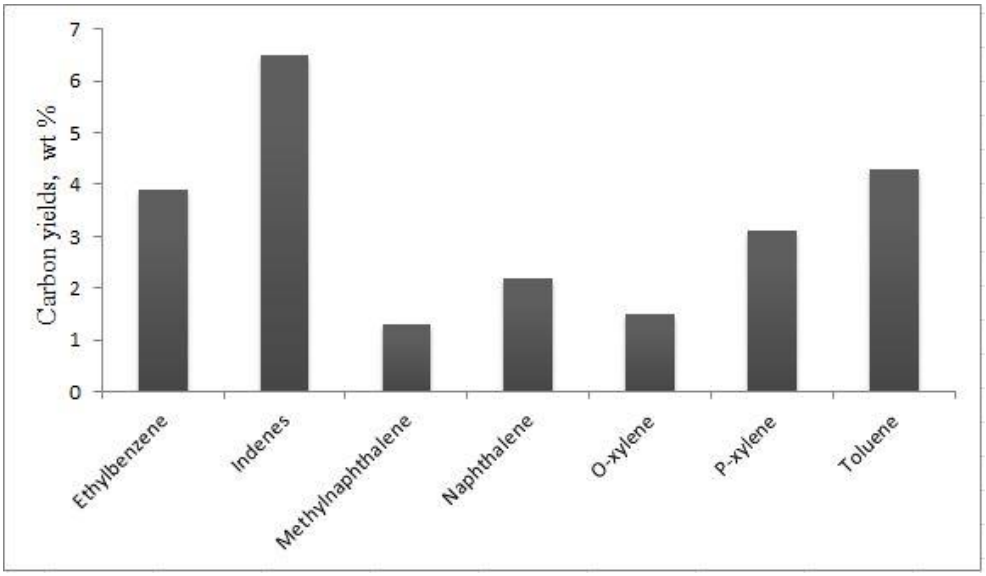

Fig. 3. Carbon yields of the aromatic hydrocarbons from co-pyrolysis in the presence HZSM-5/γ-Al_2O_3/Na_2CO_3 at 700 °C

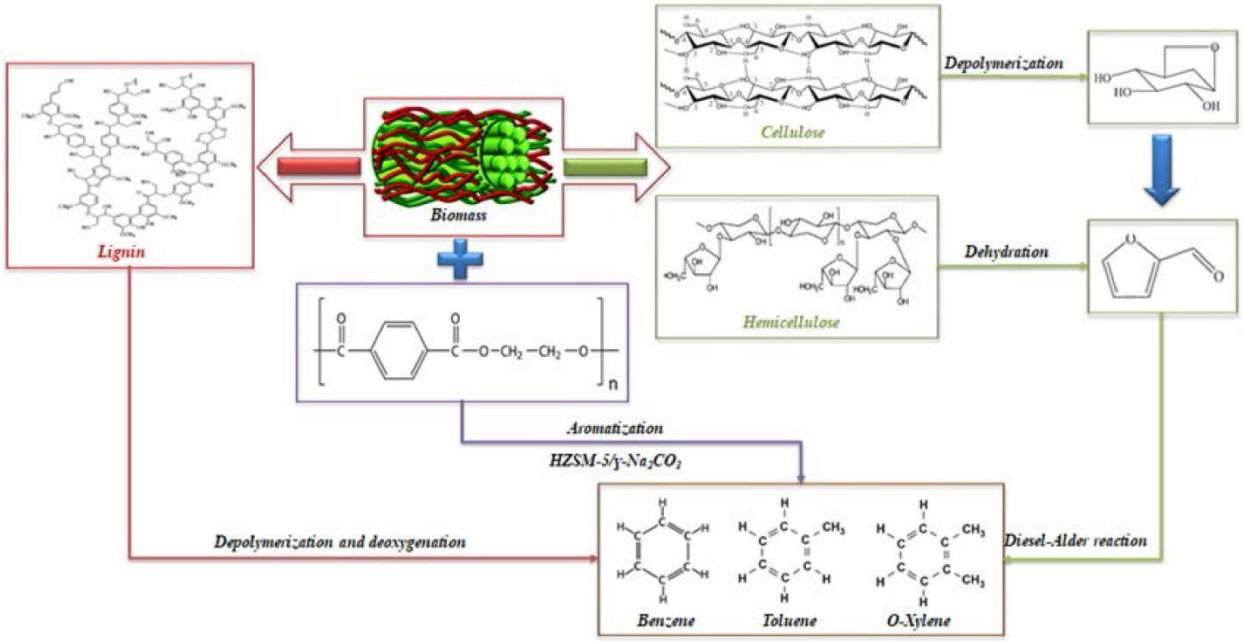

Fig. 4. The co-pyrolysis reaction pathways of biomass and PET

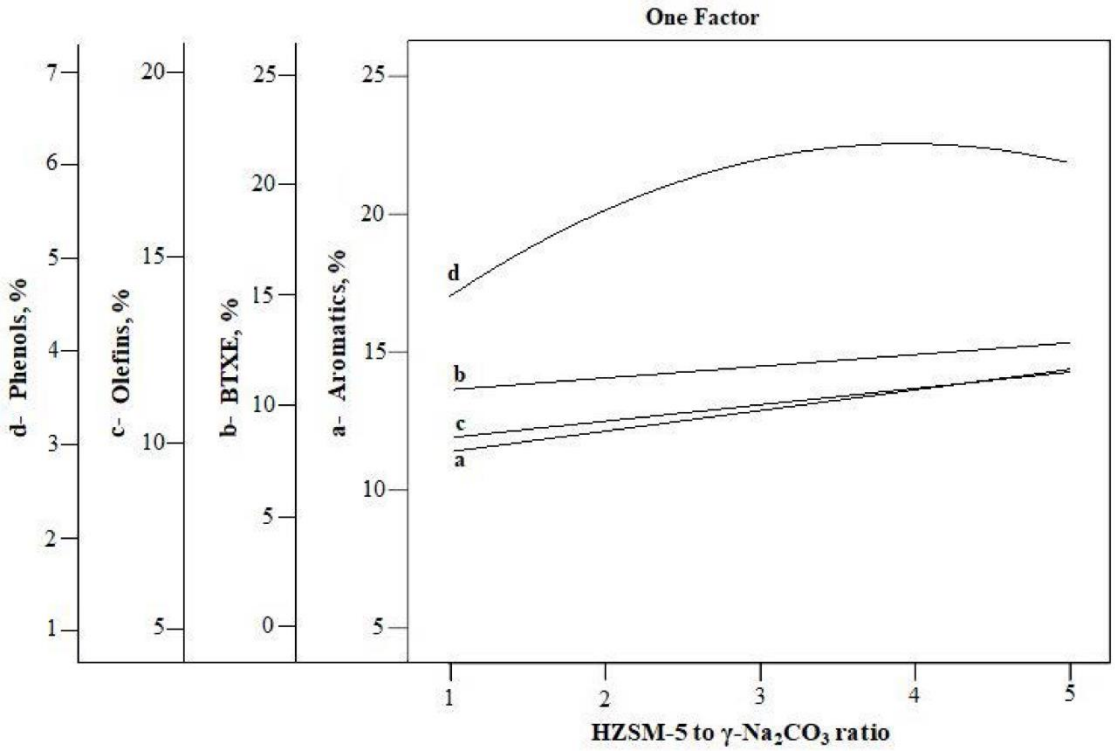

Fig. 5. The independent effect of HZSM-5 to γ-Na_2CO_3 on, a) Aromatics; b) BTXE; c) Olefins; d) Phenols

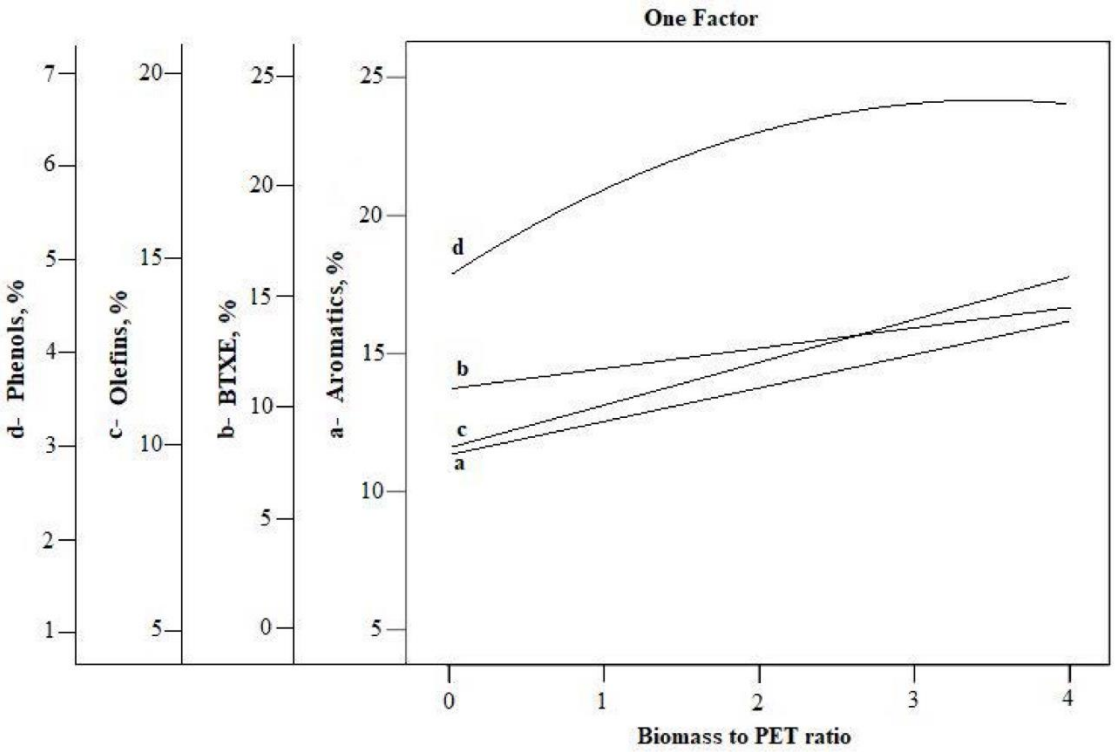

Fig. 6. The independent effect of Biomass to PET ratio on, a) Aromatics; b) BTXE; c) Olefins; d) Phenols.

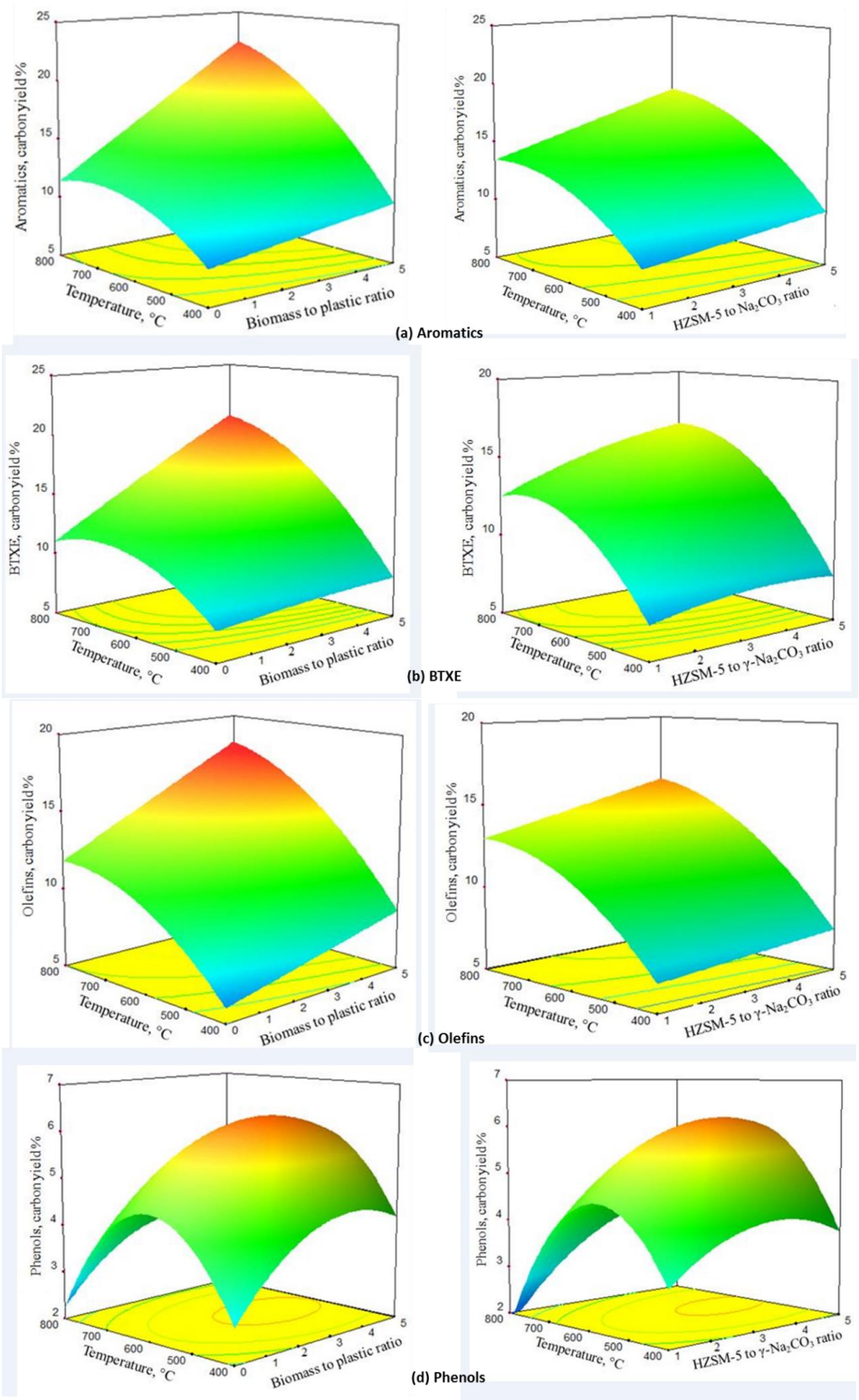

Fig. 7. The interaction between temperature, biomass to plastic ratio and HZSM-5 to γ-Na_2CO_3 on the co-pyrolysis distributions, a) Aromatics; b) BTXE; c) Olefins; d) Phenols